Received: 19 July 2020 | Revised: 29 October 2020 | Accepted: 1 November 2020

DOI: 10.1111/cas.14721

ORIGINAL ARTICLE

Cancer Science WILEY

Hemagglutinating virus of Japan-envelope containing programmed cell death-ligand 1 siRNA inhibits immunosuppressive activities and elicits antitumor immune responses in glioma

Narushi Sugii[1,2] | Masahide Matsuda[1] | Genki Okumura[3,4] | Akira Shibuya[3,5] | Eiichi Ishikawa[1] | Yasufumi Kaneda[6] | Akira Matsumura[1]

[1]Department of Neurosurgery, Faculty of Medicine, University of Tsukuba, Ibaraki, Japan

[2]Majors of Medical Sciences, Graduate School of Comprehensive Human Sciences, University of Tsukuba, Ibaraki, Japan

[3]Department of Immunology, Faculty of Medicine, University of Tsukuba, Ibaraki, Japan

[4]Majors of Biomedical Sciences, Graduate School of Comprehensive Human Sciences, University of Tsukuba, Ibaraki, Japan

[5]Life Science Center for Survival Dynamics, Tsukuba Advanced Research Alliance (TARA), R&D Center for Innovative Drug Discovery, University of Tsukuba, Ibaraki, Japan

[6]Division of Gene Therapy Science, Department of Genome Biology, Graduate School of Medicine, Osaka University, Osaka, Japan

Correspondence
Masahide Matsuda, Department of Neurosurgery, Faculty of Medicine, University of Tsukuba, Tsukuba, Ibaraki 305-8575, Japan.
Email: m-matsuda@md.tsukuba.ac.jp

Funding information
Grants-in-Aid for Scientific Research (KAKENHI), Grant/Award Number: JP18K08988

Abstract

The programmed cell death-1/programmed cell death-ligand 1 (PD-1/PD-L1) pathway is involved in preventing immune system-mediated destruction of malignant tumors including glioblastoma. However, the therapeutic influence of PD-1/PD-L1 inhibition alone in glioblastoma is limited. To develop effective combination therapy involving PD-1/PD-L1 inhibition, we used a non-replicating virus-derived vector, hemagglutinating virus of Japan-envelope (HVJ-E), to inhibit tumor cell PD-L1 expression by delivering siRNA targeting PD-L1. HVJ-E is a promising vector for efficient delivery of enclosed substances to the target cells. Moreover, HVJ-E provokes robust antitumoral immunity by activating natural killer (NK) cells and cytotoxic T lymphocytes (CTLs), and by suppressing regulatory T lymphocytes (Treg). We hypothesized that we could efficiently deliver PD-L1-inhibiting siRNAs to tumor cells using HVJ-E, and that synergistic activation of antitumoral immunity would occur due to the immunostimulating effects of HVJ-E and PD-1/PD-L1 inhibition. We used artificially induced murine glioma stem-like cells, TS, to create mouse (C57BL/6N) glioblastoma models. Intratumoral injection of HVJ-E containing siRNA targeting PD-L1 (siPDL1/HVJ-E) suppressed the expression of tumor cell PD-L1 and significantly suppressed tumor growth in subcutaneous models and prolonged overall survival in brain tumor models. Flow cytometric analyses of brain tumor models showed that the proportions of brain-infiltrating CTL and NK cells were significantly increased after giving siPDL1/HVJ-E; in contrast, the rate of Treg/$CD4^+$ cells was significantly decreased in HVJ-E-treated tumors. CD8 depletion abrogated the therapeutic effect of siPDL1/HVJ-E, indicating that $CD8^+$ T lymphocytes mainly mediated this therapeutic effect.

Abbreviations: CXCL, C-X-C motif chemokine ligand; DC, dendritic cell; GBM, glioblastoma; HAU, hemagglutinating unit; HVJ-E, hemagglutinating virus of Japan-envelope; ICI, immune checkpoint inhibitor; IFN, interferon; IHC, immunohistochemistry; IL, interleukin; MFI, mean fluorescence intensity; NK, natural killer; OS, overall survival; PD-1, programmed cell death-1; PD-L1, programmed cell death-ligand 1; siNC, negative control of small interfering ribonucleic acid; siPDL1, small interfering ribonucleic acid targeting programmed cell death-ligand 1; TME, tumor microenvironment; Treg, regulatory T lymphocyte.

We believe that this non-replicating immunovirotherapy may be a novel therapeutic alternative to treat patients with glioblastoma.

KEYWORDS
glioblastoma, hemagglutinating virus of Japan-envelope, immune checkpoint, regulatory T lymphocyte, siRNA

1 | INTRODUCTION

Glioblastoma (GBM) is a devastating disease with a median OS time of fewer than 20 months.[1,2] Although treatment modalities including surgery, radiotherapy, and chemotherapy have improved, curing GBM remains challenging, highlighting an urgent need to develop novel therapeutic strategies from different perspectives. In recent years, the immune system has been found to play critical roles in combating tumors; however, malignant tumors including GBM avoid immune destruction by creating an immunosuppressive tumor microenvironment (TME) via induction of immunosuppressive cytokines, expression of immune checkpoint molecules, and recruitment of immunosuppressive cells such as Treg.[3-6]

Programmed cell death-1 (PD-1) is an immune checkpoint molecule expressed on the cell surface of activated lymphocytes. When PD-1 binds with its ligand, programmed cell death-ligand 1 (PD-L1), an inhibitory signal is transduced, and immune cells become inactivated or exhausted. Malignant tumors, including GBM, abundantly express PD-L1[7,8] and, thus, most lymphocytes in the TME can become exhausted through this immuno-inhibitory pathway. Recently, several immune checkpoint inhibitor (ICI) targeting the PD-1/PD-L1 pathway have been developed; they restore the function of inactivated immune cells and show therapeutic effects on many types of malignant tumors.[9,10] However, the therapeutic influence of ICI on brain tumors remains to be elucidated.[11] The brain is protected by the blood-brain barrier, which is a structural barrier that prevents substances with sizeable molecular weights from penetrating into the brain parenchyma. All ICI currently available are antibody drugs and have very high molecular weights;[12] thus, an adequate amount of ICI cannot reach the tumor site.[13] Also, GBM is thought to have relatively low immunogenicity,[14,15] indicating that inhibition of the PD-1/PD-L1 axis alone is not sufficient to produce the potential benefit of antitumor immunity. Therefore, to elicit the maximum benefit of ICI against brain tumors, we need a unique delivery system for ICI, and ICI should be combined with additional immunostimulating agents.

To overcome these problems, we focused on a non-replicating virus-derived vector, named hemagglutinating virus of Japan-envelope (HVJ-E). HVJ-E is a replication-defective inactivated virus particle made from Sendai virus (HVJ) that was treated with ultraviolet irradiation to destroy the viral genome RNA.[16] Although HVJ-E is inactivated, the viral envelope can fuse with target cells and deliver agents into the target cells. HVJ-E can be loaded with various types of molecules, such as RNA, DNA, and proteins, and efficiently deliver them to the cytoplasm of target cells. We have reported promising antitumoral effects of HVJ-E containing therapeutic siRNA against mouse brain glioma models in vivo.[17] Moreover, another notable feature is that HVJ-E itself provokes strong antitumoral immunity by activating NK cells and CTL, inducing them to infiltrate the tumor site, and also by suppressing Treg in an IL-6-dependent manner.[18-21]

Thus, we hypothesized that we could efficiently deliver PD-L1-inhibiting agents to tumor cells using HVJ-E as a vector and, moreover, the synergistic effects of antitumor immunity would be obtained via the immunostimulating effects of HVJ-E itself and immune checkpoint inhibition. To test these hypotheses, we created subcutaneous/brain GBM models in mice and administered HVJ-E containing siRNA targeting PD-L1, and showed potent antitumoral effects of this combination therapy.

2 | MATERIALS AND METHODS

2.1 | Cell line and mice

We used an induced murine glioma stem-like cell line, TS, which was originally established and kindly provided by Dr Hideyuki Saya (Division of Gene Regulation, Keio University School of Medicine, Tokyo, Japan). Briefly, primary tumors were established by orthotopic implantation of Ink 4a/Arf$^{-/-}$ neural stem and progenitor cells expressing GFP-tagged human HRasV12 into the brain of wild-type mice. Then, TS cells were isolated from the primary tumors and sorted by fluorescence due to GFP with flow cytometry.[22] TS cells were maintained in neural stem cell medium, consisting of DMEM-F-12 (D8437; Sigma-Aldrich, St Louis, MO, USA) supplemented with recombinant human epidermal growth factor (20 ng/mL) (PeproTech, Rocky Hill, NJ, USA), recombinant human basic fibroblastic growth factor (20 ng/mL) (PeproTech), B27 supplement without vitamin A (Thermo Fisher Scientific, Waltham, MA, USA), heparan sulfate (200 ng/mL) (Amsbio, Oxfordshire, UK), and penicillin (100 U/mL)-streptomycin (100 ng/mL) (P0781; Sigma-Aldrich). Cells were incubated at 37°C in a humidified atmosphere of 95% air and 5% CO_2. Female C57BL/6N specific pathogen-free mice aged 5-6 weeks were purchased from Japan SLC, Inc. (Shizuoka, Japan) and maintained in a temperature-controlled, pathogen-free room. All animals were handled according to the approved protocols and the guidelines of the Laboratory Animal Resource Center of the University of Tsukuba (approval numbers from 2017 to 2020 were 17-122, 18-010, 19-015, and 20-024, respectively). All efforts were made to minimize animal suffering.

2.2 | siRNA targeting PD-L1 mRNA

We purchased predesigned siRNA targeting PD-L1 mRNA (MISSION siRNA SASI_Mm02_00326460) from Sigma-Aldrich Japan (Tokyo, Japan). The sequences of this siRNA are 5′-CUUCUG AGCAUGAACUAAUTT-3′ (sense) and 5′-AUUAGUUCAUGCUCAGA AGTT-3′ (antisense). We also purchased MISSION siRNA Universal Negative Control (SIC-001-50, Sigma-Aldrich Japan) for the negative control, the sequence of which is not available. siRNAs were mixed with PBS to a final concentration of 50 μM.

2.3 | Preparation of HVJ-E

Hemagglutinating virus of Japan (VR-105 parainfluenza1 Sendai/52, Z strain) was purchased from ATCC (Manassas, VA, USA), amplified in the chorioallantoic fluid of 10- to 14-day-old chick eggs, purified by centrifugation, and inactivated by exposure to ultraviolet irradiation (99 mJ/cm^2) as previously described.[16]

2.4 | Hemagglutinating virus of Japan-envelope vector-mediated siRNA transfection

HVJ-E suspended in PBS was used for each transfection in the present study. In all, 10 μL of the HVJ-E suspension (100 hemagglutinating units [HAU]) was mixed with 1 μL of 50 μM siRNA solution, 4.5 μL of 3% (v/v) Triton X-100 (final concentration 0.2%), and 52 μL of PBS, as previously described with slight modifications.[16,17] After 5 min of incubation at 4°C, the mixture was centrifuged (17,700 *g*) for 5 min at 4°C. After this, the pellet was washed once with 300 μL PBS to remove the detergent and unincorporated siRNA. Then, HVJ-E containing siRNA was resuspended in PBS.

2.5 | Subcutaneous tumor model

We made subcutaneous tumor models to evaluate the changes in tumor volume over time (Figure 1A). Mice were anesthetized with an intraperitoneal injection of 80 mg/kg ketamine (Daiichi Sankyo Company Ltd, Tokyo, Japan) and 10 mg/kg xylazine (Bayer Japan, Osaka, Japan). Viable TS cells (5×10^5) were re-suspended in 100 μL PBS and injected into the subcutaneous space in the back of each mouse. Tumor cell-inoculated mice were randomly divided into three groups: siPDL1/HVJ-E group (treated with HVJ-E containing siRNA targeting PD-L1); siNC/HVJ-E group (HVJ-E containing negative control siRNA); control group (PBS only). On days 4, 7, and 10, 100 μL PBS or HVJ-E containing siRNA (200 HAU) suspended in 100 μL PBS was injected into the tumors. HVJ-E containing siRNA was prepared as described above. Tumor size was measured with slide calipers every 3-4 days, and tumor volume was calculated with the following formula: tumor volume (mm^3) = length × (width)^2/2. When the tumor

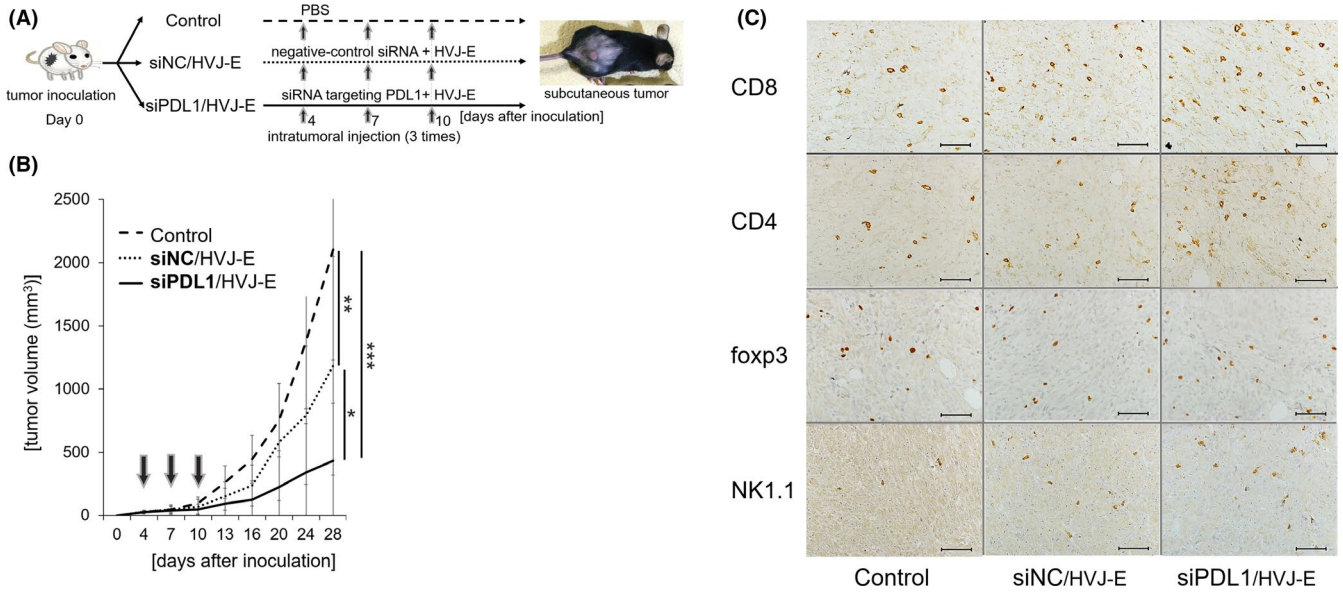

FIGURE 1 siPDL1/HVJ-E administration showed antitumor effects in subcutaneous tumor models with altered immune cell infiltration. Mice bearing subcutaneous tumors were divided into three groups: the control group (treated with PBS), siNC/HVJ-E group (treated with HVJ-E containing negative control siRNA), and siPDL1/HVJ-E group (treated with HVJ-E containing siRNA targeting PD-L1) (A). The therapeutic agents were injected intratumorally on days 4, 7, and 10 (black arrows on B). The mean tumor volume at 28 days after tumor cell inoculation of the siPDL1/HVJ-E group is significantly smaller than that of the other two groups (mean tumor volume ± SD) (B). Cumulative data from three independent sets of experiments were analyzed; the numbers of mice were 10 in the control group and 15 each in the other two groups. Immunohistochemistry staining of subcutaneous tumors indicates an increasing number of tumor-infiltrating CD8$^+$ T lymphocytes in the siPDL1/HVJ-E group (C). The tumor samples from each group (n = 3 each) were extracted 12 days after tumor cell inoculation. Scale bars represent 50 μm. *$P < .05$, **$P < .01$, ***$P < .001$. HVJ-E, hemagglutinating virus of Japan-envelope; PD-L1, programmed cell death-ligand 1; siNC, negative control siRNA; siPDL1, siRNA targeting PD-L1

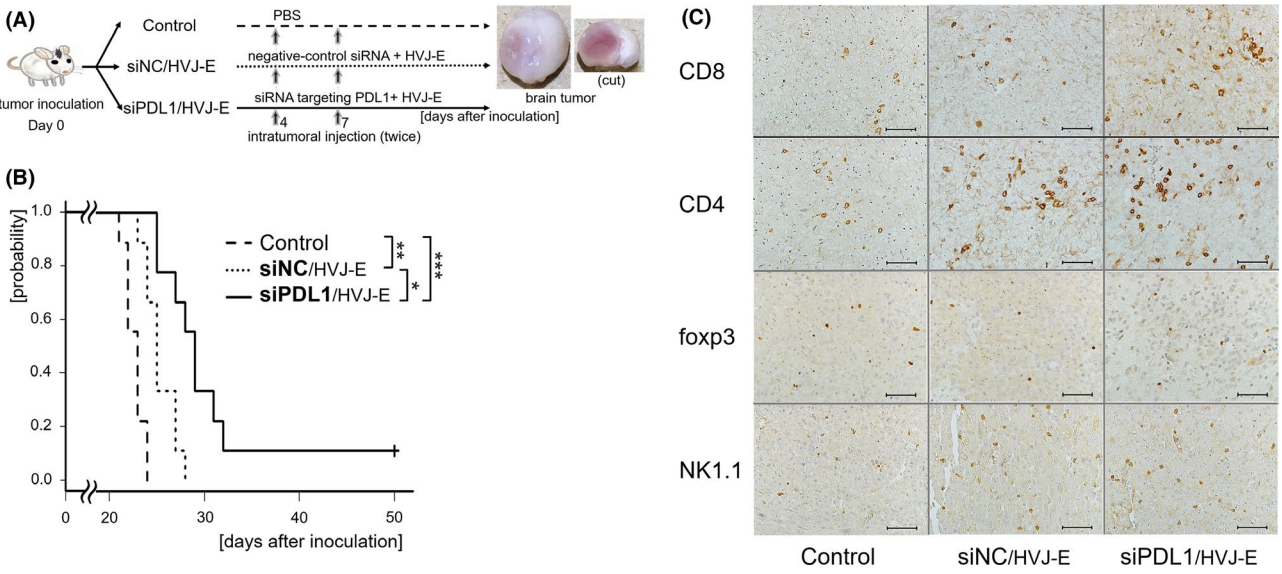

FIGURE 2 siPDL1/HVJ-E administration significantly prolonged overall survival (OS) in brain tumor models with altered immune cell infiltration. Mice with brain tumors were divided into three groups: the control group (treated with PBS), siNC/HVJ-E group (treated with HVJ-E containing negative control of siRNA), and siPDL1/HVJ-E group (treated with HVJ-E containing siRNA targeting PD-L1) (A). The therapeutic agents were given intratumorally on days 4 and 7. The survival curve shows that OS in the siPDL1/HVJ-E group is significantly longer than that in the other two groups (vs control, ***$P < .001$; vs siNC/HVJ-E, *$P < .05$) (B). Cumulative data from three independent sets of experiments were analyzed. Total numbers of mice were 10 in each group. Immunohistochemical staining of brain tumors indicates that tumor infiltration by $CD8^+$ T lymphocytes seems to increase in the siPDL1/HVJ-E group (C). Brains from each group (n = 3) were extracted 20 days after tumor cell inoculation. Scale bars represent 50 μm. *$P < .05$, **$P < .01$, ***$P < .001$. HVJ-E, hemagglutinating virus of Japan-envelope; PD-L1, programmed cell death-ligand 1

volume reached >2500 mm^3, the mouse was killed. Cumulative data from three independent sets of experiments were analyzed.

2.6 | Brain tumor model

We made brain tumor models to compare the survival time among groups (Figure 2A). Mice were anesthetized with an intraperitoneal injection of ketamine (80 mg/kg) and xylazine (10 mg/kg) and placed in a stereotaxic instrument (SR-5M-HT/SM-15R/IMS-3; Narishige Japan, Tokyo, Japan). After scalp incision, a single trepanation was carried out with a 26-gauge needle at 0.3 mm posterior to the bregma and 2.5 mm lateral to the midline. Then, 4×10^3 viable TS cells in 4 μL PBS were injected stereotactically over 2 minutes at a depth of 2.5 mm below the cortical surface using a Hamilton syringe (701RN; Hamilton, Reno, NV, USA) with a 26-gauge needle. Tumor cell-inoculated mice were randomly divided into three groups. On days 4 and 7 under anesthesia, 6 μL PBS or HVJ-E containing siRNA (200 HAU) in 6 μL PBS was injected into the tumor site using the same coordinates on the stereotactic frame. The mice were killed when they became lethargic and lost over 30% of their weight. Cumulative data from three independent sets of experiments were analyzed.

2.7 | Western blot analysis

PD-L1 protein levels were evaluated with western blot analysis. Tumor tissues from subcutaneous models were extracted 11 days after tumor cell inoculation. Each tissue lysate (50 μL/lane) was electrophoresed on SDS-PAGE. After transfer onto a PVDF membrane, the membrane was incubated for 1 hour with blocking buffer, followed by overnight incubation at 4°C with primary antibodies (Table S1). The membrane was washed with wash buffer and labeled with HRP-conjugated secondary antibodies at room temperature for 1 hour. Blotted proteins were detected using the LAS-4000 system (Fujifilm, Tokyo, Japan) and Luminata Forte Western HRP substrate (Merck, Darmstadt, Germany) according to the manufacturers' instructions. Quantification measurement was done using ImageJ version 1.53c (National Institutes of Health, Bethesda, MD, USA).

2.8 | Immunohistochemistry

For subcutaneous tumor models, three tumor-bearing mice of each group were killed 12 days after tumor cell inoculation, and the tumors were extirpated. For brain tumor models, three tumor-bearing mice of each group were killed 20 days after inoculation, and perfusion fixation with PBS and 10% formalin was done before brain extraction. Formalin-fixed and paraffin-embedded blocks of all tumor specimens were prepared and cut into 3-μm thick slices. Heat-mediated antigen retrieval was carried out with citrate buffer (pH 6.0) for anti-foxp3 and anti-CD161 antibodies or with Tris-EDTA buffer (pH 9.0) for other antibodies. Sections were incubated overnight with primary antibodies (Table S1) at 4°C. The next day, the sections were quenched in 0.3% H_2O_2 in 80% methanol for 30 minutes and then processed using the

LSAB2 System-HRP (Agilent Technologies Japan, Tokyo, Japan) followed by the Liquid DAB + Substrate Chromogen System (Agilent Technologies Japan) according to the manufacturer's instructions.

2.9 | Flow cytometry of harvested brain samples

Tumor-bearing mice were killed 20 days after tumor cell inoculation. After perfusion with PBS, the brains were dissected and homogenized in RPMI-1640 (Sigma-Aldrich) using a Tissue Grinder (Wheaton, Millville, NJ, USA). Selective isolation of leukocytes was carried out using a Percoll density gradient (GE Healthcare, Chicago, IL, USA). Cells between the 70% and 30% layers of the gradient were collected. Single-cell suspensions were treated with Fc block (2.4G2; Tonbo Biosciences, San Diego, CA, USA) and then stained with labeled anti-mouse primary antibodies diluted in a mixture of 2% FBS and propidium iodide (PI) (1:2000; Sigma-Aldrich) in PBS. Fixation and permeabilization were carried out with BD Cytofix/Cytoperm (BD Biosciences, Franklin Lakes, NJ, USA) only for foxp3 staining. Primary antibodies used in this study are shown in Table S1. Appropriate isotype controls were used, and cells were examined on a BD LSRFortessa system (BD Biosciences). Nonviable cells were excluded by forward versus side scatter analysis and fluorescence of PI. All data were analyzed using FlowJo software version 10.6.2 (FlowJo LLC, Ashland, OR, USA).

2.10 | Depletion study of CD8$^+$ T lymphocytes

Mice bearing tumors in the brain were given intraperitoneal injections of anti-CD8 antibody (clone 2.43; Bio X Cell, West Lebanon, NH, USA) at 400 μg per mouse on post-implantation day 4 and 200 μg on days 7 and 14.

2.11 | Statistical analyses

We used one-way analysis of variance to compare the volume of subcutaneous tumors and the proportion of leukocytes in flow cytometry; post-hoc tests were done with the Tukey-Kramer method. For the survival period in the brain tumor models, statistical analyses were carried out using the Kaplan-Meier method; the log-rank test adjusted with Holm's method was used to assess group differences. All statistical analyses were carried out with EZR version 1.40 (Saitama Medical Center, Saitama, Japan), which is a graphical user interface for R commander version 2.5-1/R version 3.5.2 (The R Foundation for Statistical Computing, Vienna, Austria).[23] The probability value of <0.05 was considered statistically significant.

3 | RESULTS

3.1 | Hemagglutinating virus of Japan-envelope containing siRNA targeting PD-L1 suppressed the expression of tumor PD-L1 in vivo

To confirm whether siPDL1/HVJ-E could knock down the expression of tumor PD-L1, we created subcutaneous tumor models, treated them with three injections of siPDL1/HVJ-E, and extracted proteins from tumor tissues 11 days after tumor cell inoculation for western blotting. We also obtained tumor samples on day 12 for IHC. Western blot analysis showed that the level of PD-L1 protein in tumors treated with siPDL1/HVJ-E reduced almost by half compared with those treated with PBS or siNC/HVJ-E (Figure 3A). IHC staining of subcutaneous tumor tissues also showed a decreased level of PD-L1 protein expression in the siPDL1/HVJ-E group (Figure 3B).

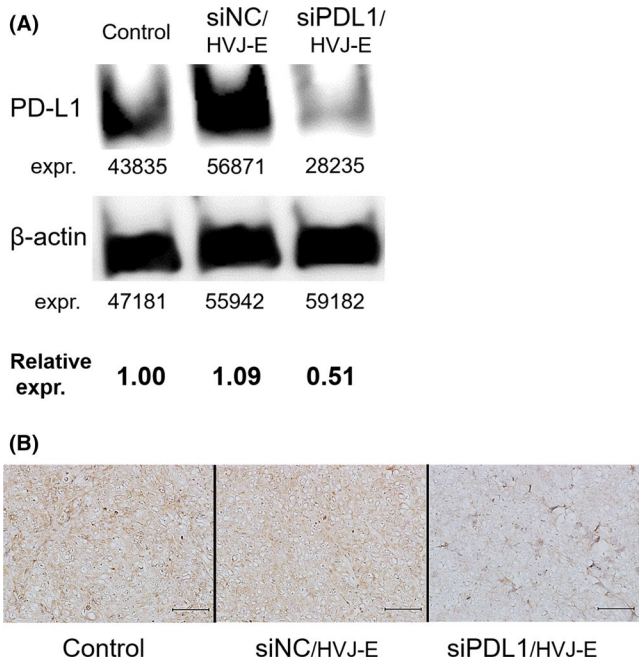

FIGURE 3 Knockdown of tumor programmed cell death-ligand 1 (PD-L1) expression by hemagglutinating virus of Japan-envelope (HVJ-E) containing siRNA targeting PD-L1 in subcutaneous tumor models. The image of western blotting and the relative expression level of PD-L1 protein (A) show that PD-L1 protein expression in the siPDL1/HVJ-E group is lower by approximately 50% than that in the other two groups. Decreased level of PD-L1 expression in the siPDL1/HVJ-E group is also seen in immunohistochemistry (B). The tumor specimens were extracted from mouse subcutaneous glioma models on post-inoculation day 11 for western blotting and on day 12 for immunohistochemistry. The tumor-bearing mice in the control group, siNC/HVJ-E group, and siPDL1/HVJ-E group were treated with PBS, HVJ-E containing negative control siRNA, and HVJ-E containing siRNA targeting PD-L1, respectively. Scale bars represent 50 μm. expr., expression; siNC, negative control siRNA; siPDL1, siRNA targeting PD-L1

Thus, we confirmed that siPDL1/HVJ-E knocked down the expression of PD-L1 in tumors in vivo.

3.2 | Combination of HVJ-E and siRNA-mediated PD-L1 knockdown suppressed tumor growth in the subcutaneous tumor model

To evaluate the therapeutic influence of siPDL1/HVJ-E, we created subcutaneous tumor models by injecting glioma stem-like cells, TS cells, in the backs of mice. The mice were divided into three groups (Figure 1A): the siPDL1/HVJ-E group (HVJ-E containing siRNA targeting PD-L1), which was used to evaluate the combined effects of PD-L1 blockade and HVJ-E; the siNC/HVJ-E group (treated with HVJ-E containing negative control siRNA), which was used to monitor the efficacy of HVJ-E alone; and the control group (PBS only). We followed the changes in tumor volume over time (Figure 1B). Mean tumor volumes at 28 days after tumor cell inoculation in the siPDL1/HVJ-E, siNC/HVJ-E, and control groups were 432.8, 1174.0, and 2103.9 mm^3, respectively ($P < .001$). Post-hoc tests showed that the tumor volume in the siPDL1/HVJ-E group was significantly smaller than that in the siNC/HVJ-E group ($P < .05$). Next, we carried out IHC staining of subcutaneous tumor samples and assessed tumor-infiltrating lymphocytes. The number of $CD8^+$ T lymphocytes was increased in siPDL1/HVJ-E-treated tumors (Figure 1C).

3.3 | Combination of HVJ-E and siRNA-mediated PD-L1 knockdown prolonged OS time in the mouse brain tumor model

We created brain tumor models in mice to elucidate the therapeutic effects of siPDL1/HVJ-E. Tumor cells were stereotactically inoculated into the right hemisphere, and therapeutic agents were injected intratumorally on days 4 and 7 (Figure 2A). Median OS times of the siPDL1/HVJ-E, siNC/HVJ-E, and control groups were 28, 26, and 22.5 days, respectively ($P < .001$) (Figure 2B). siPDL1/HVJ-E administration significantly prolonged OS time compared with the siNC/HVJ-E ($P < .05$) and control groups ($P < .001$). Then, we killed three mice from each group on day 20 for IHC staining; tumor-infiltrating $CD8^+$ T lymphocytes were increased in the siPDL1/HVJ-E group and $CD4^+$ T lymphocytes were increased in the siNC/HVJ-E and the siPDL1/HVJ-E groups (Figure 2C).

3.4 | Combination of HVJ-E and siRNA-mediated PD-L1 knockdown increased the proportions of brain-infiltrating $CD8^+$ T lymphocytes and NK cells

To understand the mechanism of the antitumoral effects of siPDL1/HVJ-E against the brain tumors, we extracted the brains of tumor-bearing mice on post-inoculation day 20 and performed flow cytometry to evaluate brain-infiltrating leukocytes. After gating each leukocyte population (Figures S1, S2), we compared the proportions of brain-infiltrating $CD8^+$ T lymphocytes ($CD45.2^+$ $CD3^+$ $CD11b^-$ $CD8^+$ $CD4^-$), $CD4^+$ T lymphocytes ($CD45.2^+$ $CD3^+$ $CD11b^-$ $CD8^-$ $CD4^+$), NK cells ($CD45.2^+$ $CD3^-$ $CD11b^{dim}$ $NK1.1^+$), Tregs ($CD45.2^+$ $CD3^+$ $CD11b^-$ $CD8^-$ $CD4^+$ $foxp3^+$), macrophages ($CD45.2^+$ $CD11b^+$ $F4/80^+$ $Ly6C^+$ $CX_3CR_1^-$), and M2 macrophages ($CD45.2^+$ $CD11b^+$ $F4/80^+$ $Ly6C^+$ $CX_3CR_1^-$ $CD206^+$). The proportions of brain-infiltrating $CD8^+$ and NK cells per $CD45.2^+$ leukocytes (all leukocytes) were significantly increased in the siPDL1/HVJ-E group compared with the other two groups (Figure 4A) (vs siNC/HVJ-E, $P < .05$; vs control, $P < .001$). The brain-infiltrating $CD4^+$ T lymphocytes seemed to increase after siPDL1/HVJ-E administration, but the difference was not significant compared to siNC/HVJ-E. In contrast, the proportions of Treg among $CD4^+$ T lymphocytes were significantly lower in the two groups with HVJ-E administration (siPDL1/HVJ-E and siNC/HVJ-E groups); siNC/HVJ-E and siPDL1/HVJ-E showed similar results regarding the Treg proportion. The proportion of M2 macrophages, known to have immunosuppressive properties, in the macrophage population was almost the same between the three groups. These observations suggested that the therapeutic effect of siPDL1/HVJ-E was mediated by an increase in $CD8^+$ T lymphocytes and NK cells and a decrease in the Treg proportion. Then, we evaluated the expression levels of PD-1 on the lymphoid cells. The PD-1 molecules were abundantly expressed on $CD8^+$ T lymphocytes and $CD4^+$ T lymphocytes, moderately on Tregs, but little on NK cells (Figure 4B; S3).

3.5 | Therapeutic effects of siPDL1/HVJ-E were dependent on $CD8^+$ T lymphocytes

We carried out CD8 depletion to evaluate the contributions of $CD8^+$ T lymphocytes. Intraperitoneal injections of anti-CD8 antibody entirely ablated $CD8^+$ T lymphocytes but not for other cell fractions (Figure 5A). We divided brain tumor-bearing mice into the siPDL1/HVJ-E and the siNC/HVJ-E groups. CD8 depletion abrogated the difference in OS time between the two groups, indicating that $CD8^+$ T lymphocytes mediated the combinational therapeutic effect of PD-L1 blockade and HVJ-E (Figure 5B).

4 | DISCUSSION

In the present study, we delivered siRNA targeting PD-L1 into tumor cells using HVJ-E as a vector and found reduced expression of PD-L1 in tumors in vivo. siPDL1/HVJ-E showed significant antitumoral effects both in the subcutaneous and brain GBM models. Based on the results of flow cytometry, siPDL1/HVJ-E administration induced effector lymphocytes such as $CD8^+$ T lymphocytes, $CD4^+$ T lymphocytes, and NK cells to infiltrate the tumor sites. In contrast, the proportion of Treg among $CD4^+$ T lymphocytes was significantly lower in the two groups with HVJ-E administration. These alterations in

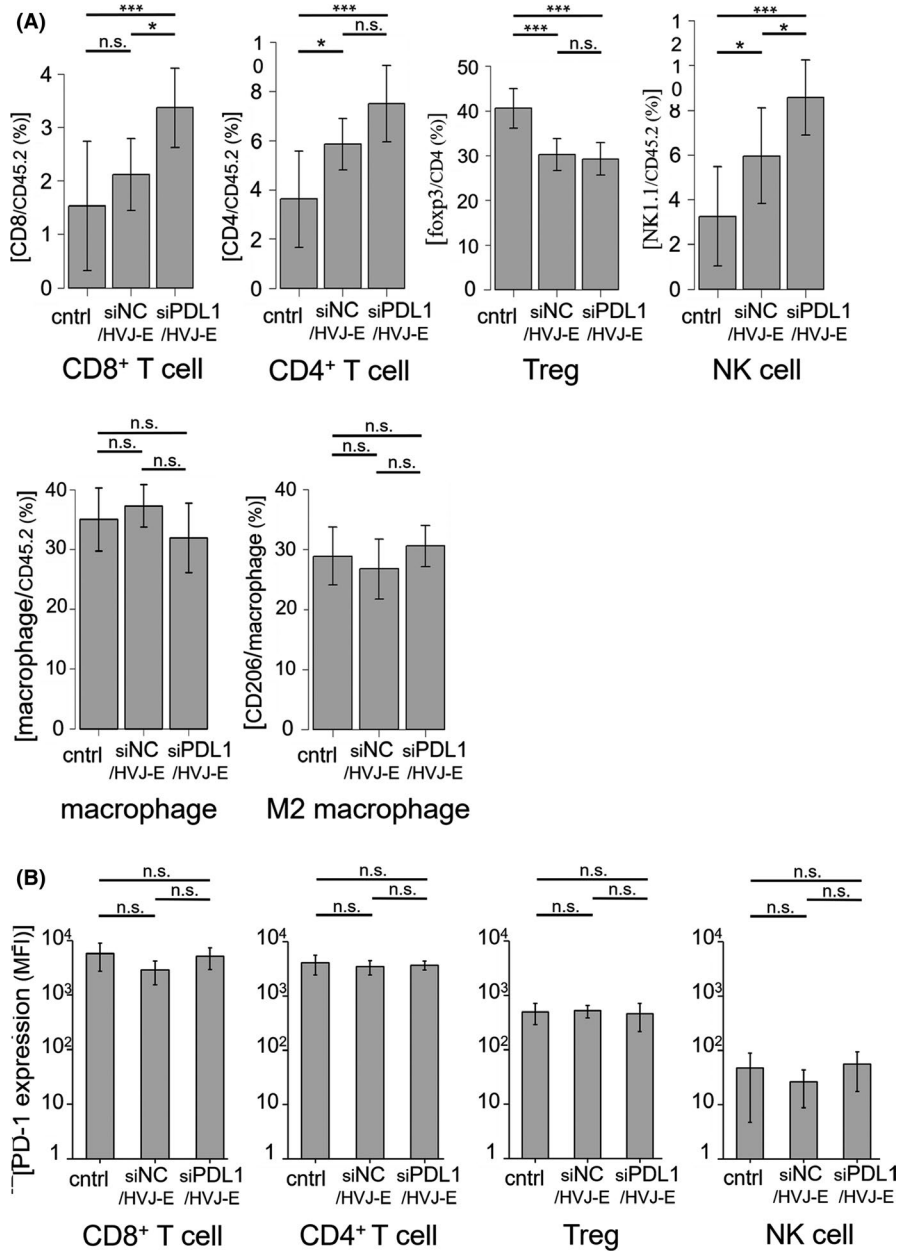

FIGURE 4 Proportions of brain-infiltrating $CD8^+$ T lymphocytes and natural killer (NK) cells significantly increased after giving siPDL1/HVJ-E. We extracted brain samples from each group (n = 10 each for lymphoid cells and n = 7 each for myeloid cells) 20 days after tumor cell inoculation. We evaluated the brain-infiltrating leukocytes with flow cytometry. Each leukocyte fraction was defined as follows (Figures S1, S2): $CD8^+$ T lymphocytes ($CD45.2^+$ $CD3^+$ $CD11b^-$ $CD8^+$ $CD4^-$), $CD4^+$ T lymphocytes ($CD45.2^+$ $CD3^+$ $CD11b^-$ $CD8^-$ $CD4^+$), NK cells ($CD45.2^+$ $CD3^-$ $CD11b^{dim}$ $NK1.1^+$), Treg ($CD45.2^+$ $CD3^+$ $CD11b^-$ $CD8^-$ $CD4^+$ $foxp3^+$), macrophages ($CD45.2^+$ $CD11b^+$ $F4/80^+$ $Ly6C^+$ $CX_3CR_1^-$), and M2 macrophages ($CD45.2^+$ $CD11b^+$ $F4/80^+$ $Ly6C^+$ $CX_3CR_1^-$ $CD206^+$). Brain infiltration by $CD8^+$ T lymphocytes and NK cells per $CD45.2^+$ leukocytes is significantly increased in the siPDL1/HVJ-E group compared with the other two groups. Proportions of Treg among $CD4^+$ T lymphocytes are significantly lower in the two groups with HVJ-E administration (ie, siNC/HVJ-E and siPDL1/HVJ-E groups) (A). We evaluated the expression levels of PD-1 on the lymphoid cells. Cumulative data from two independent sets of experiments are shown (B) (n = 7 in each group). $CD8^+$ and $CD4^+$ T lymphocytes, including Treg, markedly express PD-1 molecules, whereas NK cells hardly express PD-1. $^*P < .05$, $^{***}P < .001$. HVJ-E, hemagglutinating virus of Japan-envelope; MFI, mean fluorescence intensity; n.s., not significantly different; PD-1, programmed cell death-1; siNC/HVJ-E, group treated with HVJ-E containing negative control siRNA; siPDL1/HVJ-E, group treated with HVJ-E containing siRNA targeting PD-L1; Treg, regulatory T lymphocyte;

immune cell distribution may have played a critical role in the antitumor effects of this combination therapy. In particular, $CD8^+$ T lymphocytes were observed to be an essential immune cell subset as shown with the CD8 depletion study.

HVJ-E itself promotes maturation of dendritic cell (DC) and induces the production of various cytokines, such as type-I IFN, IL-6, and CXCL-10, by mature DC.[19-21] These cytokines activate NK cells and attract them to the tumor sites through CXCL-10/CXCR-3

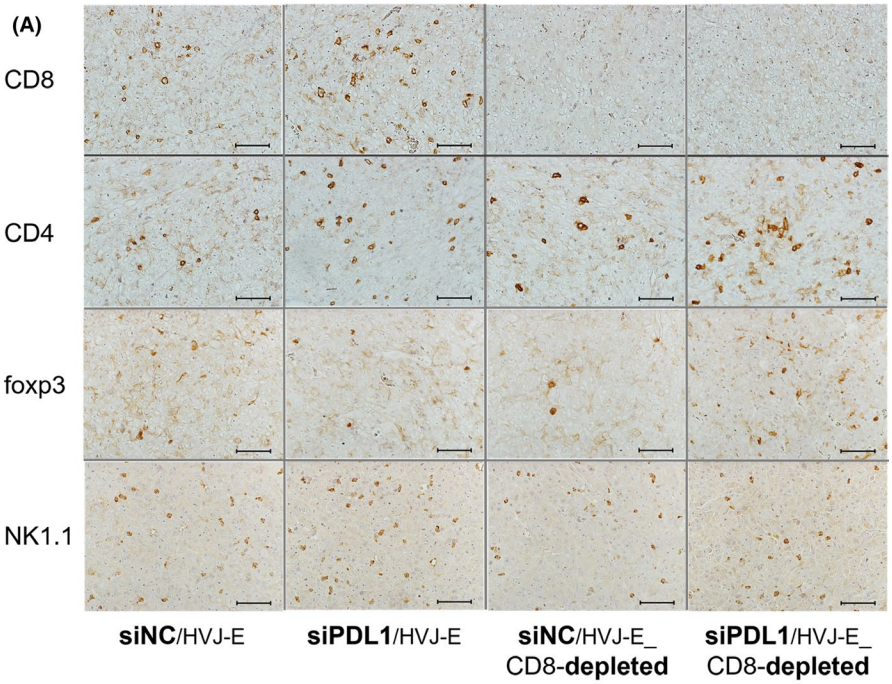

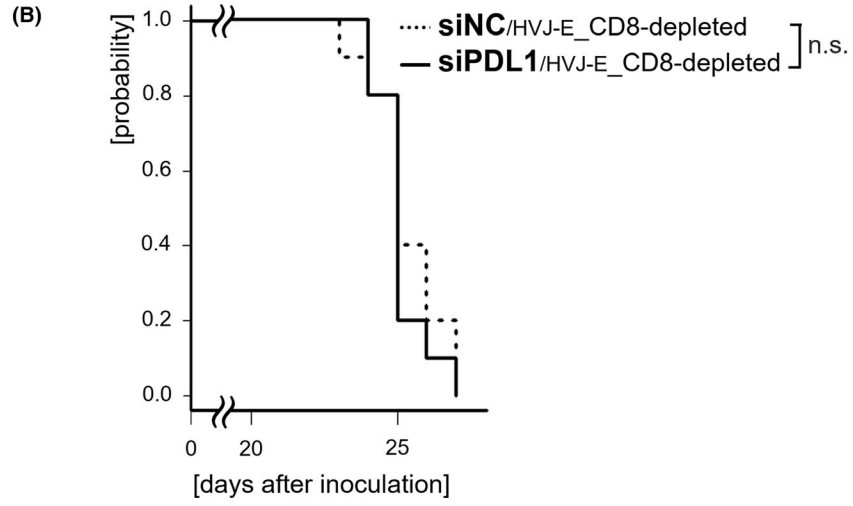

FIGURE 5 CD8 depletion abrogated the therapeutic effects of siPDL1/HVJ-E. We carried out CD8 depletion with intraperitoneal injections of anti-CD8 antibody (800 μg/mouse) and evaluated overall survival (OS) of the brain tumor-bearing mice. Immunohistochemical staining of brain tumor samples from 20 days after tumor cell inoculation shows that only $CD8^+$ T lymphocytes are entirely ablated in the anti-CD8 antibody administered groups (A). CD8 depletion abrogates the difference in OS between the siNC/HVJ-E and the siPDL1/HVJ-E groups (B) (n = 10 each). Scale bars represent 50 μm. HVJ-E, hemagglutinating virus of Japan-envelope; n.s., not significantly different; siNC/HVJ-E, group treated with HVJ-E containing negative control siRNA; siPDL1/HVJ-E, group treated with HVJ-E containing siRNA targeting PD-L1

signals, and suppress Treg in an IL-6-dependent way. Also, activated NK cells secrete high levels of IFN-γ that upregulate CXCL9-11 chemokines or cell adhesion molecules, resulting in recruitment and activation of CTL and additional NK cells, and subsequent strong antitumor immunity.[19-21,24,25] Various other viruses have been reported to have potential to induce antitumor immunity by using the natural antiviral immune response.[26] When used for viral vectors in gene therapy or engineered oncolytic viruses, these viruses commonly induce tumor antigen-specific $CD8^+$ T lymphocytes as well as NK cells.[26,27] In contrast, suppression of Treg is a comparatively unique feature to HVJ-E. Regarding IFN-γ secretion induced by HVJ-E, IFN-γ also upregulates tumor PD-L1 expression that can cause CTL exhaustion and inactivation through PD-1/PD-L1 interactions.[4,28] In terms of immunosuppression as a result of IFN-γ-dependent PD-L1 upregulation, combination treatment with siRNA-mediated PD-L1 knockdown and HVJ-E-induced antitumor immune responses may resolve this undesirable concomitant immunosuppression.

Flow cytometric analyses showed that not only $CD8^+$ T lymphocytes but also $CD4^+$ T lymphocytes and NK cells seemed to increase in the siPDL1/HVJ-E group (Figure 4A). Although NK cells potentially have intense tumoricidal activity, little is known about the relationship between the PD-1/PD-L1 axis and murine NK cells. Several previous studies have mentioned the possible enhancement of NK cell responses to tumors by PD-1/PD-L1 blockade.[29,30] However, the PD-1 expression level in NK cells is highly variable and is particularly low in mice.[30] Also, whether and how the PD-1/PD-L1 axis influences the antitumoral activity of NK cells remains debatable. Our flow cytometric data showed that an increased proportion of NK cells infiltrated the brains in the siPDL1/HVJ-E group. Nevertheless, brain-infiltrating NK cells in the present study expressed little or no PD-1 molecules (Figure 4B, S3), and thus, the underlying mechanism

for the increase in NK cells associated with siPDL1/HVJ-E treatment is indirect and may be cytokine-dependent. Further, as shown by the result of the CD8 depletion experiment, NK cells played a minimal role in the enhanced antitumoral effects of this combination therapy. Taken together, these results suggest that PD-1/PD-L1 blockade is unlikely to independently elicit antitumoral activity by NK cells in mouse brain tumors.

$CD4^+$ T lymphocytes can be either antitumoral (T helper cells) or pro-tumoral (ie, Treg). Treg is predisposed to increase in the TME compared to non-tumor circumstances.[4,5] Most Treg in the TME express PD-1 molecules on their surface,[31] and PD-1/PD-L1 inhibition functionally activates not only $CD8^+$ T lymphocytes but also Treg, which can result in hyperprogression of malignant tumors.[32] In another report, CD4 depletion may decrease the tumor volume when the PD-1/PD-L1 pathway is inhibited.[33] These data suggest that inhibiting the PD-1/PD-L1 axis without concern for Treg may be perilous. HVJ-E reduces the number of Treg and suppresses their functions in an IL-6-dependent manner through the maturation of DC,[19] indicating that HVJ-E has excellent chemistry with PD-1/PD-L1 pathway inhibition.

Although the brain was once thought to be an immune-privileged site, we now know that the immune system is active in the brain and that most human GBM express PD-L1.[7,8] Thus, PD-1/PD-L1 pathway blockade is theoretically beneficial for GBM treatment. However, the efficacy of PD-1/PD-L1 pathway inhibition in human GBM has yet to be shown.[11] A possible reason is the relatively low immunogenicity of GBM. GBM is considered to be a "cold tumor" because it has relatively low immunogenicity due to the limited number of targetable antigens from genomic mutations[34] and its immunosuppressive TME.[4,5] PD-1/PD-L1 blockade can re-activate exhausted effector immune cells, but it cannot activate naïve immune cells. Accordingly, ICI is generally considered to work better in combination with immune-stimulating therapies (such as vaccinations or viral therapies),[35,36] or enhancers of effector cell infiltration as represented by anti-angiogenic therapies.[37,38] HVJ-E can activate cells of the innate immune system such as DC and NK cells and recruit them to tumor sites, leading to the activation of acquired immunity.[19-21]

In the present study, we incorporated siRNAs into HVJ-E to suppress tumor PD-L1 expression and demonstrated the additional benefit in both subcutaneous and brain tumor mouse models. Currently, several clinical trials using HVJ-E (GEN0101, manufactured by GenomIdea, Inc., Osaka, Japan) against malignant melanoma and malignant mesothelioma are ongoing in Japan. HVJ-E is well tolerated and safe for clinical use.[39,40] Moreover, HVJ-E is more effective in human-derived tumors than in mouse-derived tumors because of the direct killing effects of HVJ-E on malignant cells by apoptosis[41] and necroptosis.[42] Therefore, we expect the combination of HVJ-E and siRNA-mediated PD-L1 knockdown therapy to be more potent for clinical use in human patients.

In summary, we used a novel approach to take full advantage of the immune-activating and Treg-suppressive features of HVJ-E itself with siRNA-mediated PD-L1 inhibition. This combination therapy showed promising therapeutic performance both in subcutaneous and brain GBM models with altered immune cell infiltration. $CD8^+$ T lymphocytes mediated the therapeutic effects. We believe this non-replicating immunovirotherapy may be a novel therapeutic alternative for treatment of patients with GBM.

ACKNOWLEDGMENTS

This work was supported in part by Grants-in-Aid for Scientific Research (KAKENHI) to MM (No. JP18K08988) from the Japan Society for the Promotion of Science.

DISCLOSURE

The authors have no conflicts of interest to declare in relation to this research and its publication.

ORCID

Masahide Matsuda https://orcid.org/0000-0003-2857-0374

REFERENCES

1. Stupp R, Taillibert S, Kanner A, et al. Effect of tumor-treating fields plus maintenance temozolomide vs maintenance temozolomide alone on survival in patients with glioblastoma: a randomized clinical trial. *JAMA*. 2017;318:2306-2316.
2. Stupp R, Mason WP, van den Bent MJ, et al. Radiotherapy plus concomitant and adjuvant temozolomide for glioblastoma. *New Engl J Med*. 2005;352:987-996.
3. Hanahan D, Weinberg RA. Hallmarks of cancer: the next generation. *Cell*. 2011;144:646-674.
4. Brown NF, Carter TJ, Ottaviani D, Mulholland P. Harnessing the immune system in glioblastoma. *Br J Cancer*. 2018;119:1171-1181.
5. Quail DF, Joyce JA. The microenvironmental landscape of brain tumors. *Cancer Cell*. 2017;31:326-341.
6. Chen DS, Mellman I. Oncology meets immunology: the cancer-immunity cycle. *Immunity*. 2013;39:1-10.
7. Xue S, Hu M, Iyer V, Yu J. Blocking the PD-1/PD-L1 pathway in glioma: a potential new treatment strategy. *J Hematol Oncol*. 2017;10:81.
8. Berghoff AS, Kiesel B, Widhalm G, et al. Programmed death ligand 1 expression and tumor-infiltrating lymphocytes in glioblastoma. *Neuro-oncology*. 2015;17:1064-1075.
9. Robert C, Schachter J, Long GV, et al. Pembrolizumab versus ipilimumab in advanced melanoma. *New Engl J Med*. 2015;372:2521-2532.
10. Brahmer J, Reckamp KL, Baas P, et al. Nivolumab versus docetaxel in advanced squamous-cell non-small-cell lung cancer. *New Engl J Med*. 2015;373:123-135.
11. Reardon DA, Brandes AA, Omuro A, et al. Effect of nivolumab vs bevacizumab in patients with recurrent glioblastoma: the checkmate 143 phase 3 randomized clinical trial. *JAMA Oncol*. 2020;6:1003-1010.
12. Janeway CA, Travers P, Walport M, Shlomchik MJ. *Immunobiology: The Immune System in Health and Disease*, 5th edn. NY: Garland Science; 2001.
13. Sweeney MD, Zhao Z, Montagne A, Nelson AR, Zlokovic BV. Blood-brain barrier: from physiology to disease and back. *Physiol Rev*. 2019;99:21-78.
14. Weenink B, French PJ, Sillevis Smitt PAE, Debets R, Geurts M. Immunotherapy in glioblastoma: current shortcomings and future perspectives. *Cancers*. 2020;12:751.
15. Colli LM, Machiela MJ, Myers TA, Jessop L, Yu K, Chanock SJ. Burden of nonsynonymous mutations among TCGA cancers and candidate immune checkpoint inhibitor responses. *Can Res*. 2016;76:3767-3772.

16. Kaneda Y, Nakajima T, Nishikawa T, et al. Hemagglutinating virus of Japan (HVJ) envelope vector as a versatile gene delivery system. *Mol Ther*. 2002;6:219-226.
17. Matsuda M, Yamamoto T, Matsumura A, Kaneda Y. Highly efficient eradication of intracranial glioblastoma using Eg5 siRNA combined with HVJ envelope. *Gene Ther*. 2009;16:1465-1476.
18. Matsuda M, Nimura K, Shimbo T, et al. Immunogene therapy using immunomodulating HVJ-E vector augments anti-tumor effects in murine malignant glioma. *J Neurooncol*. 2011;103:19-31.
19. Kurooka M, Kaneda Y. Inactivated Sendai virus particles eradicate tumors by inducing immune responses through blocking regulatory T cells. *Can Res*. 2007;67:227-236.
20. Fujihara A, Kurooka M, Miki T, Kaneda Y. Intratumoral injection of inactivated Sendai virus particles elicits strong antitumor activity by enhancing local CXCL10 expression and systemic NK cell activation. *Cancer Immunol Immunother*. 2008;57:73-84.
21. Saga K, Kaneda Y. Oncolytic Sendai virus-based virotherapy for cancer: recent advances. *Oncolytic Virother*. 2015;4:141-147.
22. Sampetrean O, Saga I, Nakanishi M, et al. Invasion precedes tumor mass formation in a malignant brain tumor model of genetically modified neural stem cells. *Neoplasia*. 2011;13:784-791.
23. Kanda Y. Investigation of the freely available easy-to-use software 'EZR' for medical statistics. *Bone Marrow Transplant*. 2013;48:452-458.
24. Taggart D, Andreou T, Scott KJ, et al. Anti-PD-1/anti-CTLA-4 efficacy in melanoma brain metastases depends on extracranial disease and augmentation of CD8(+) T cell trafficking. *Proc Natl Acad Sci USA*. 2018;115:E1540-E1549.
25. Peng W, Liu C, Xu C, et al. PD-1 blockade enhances T-cell migration to tumors by elevating IFN-gamma inducible chemokines. *Can Res*. 2012;72:5209-5218.
26. Chaurasiya S, Chen NG, Fong Y. Oncolytic viruses and immunity. *Curr Opin Immunol*. 2018;51:83-90.
27. Mitchell LA, Lopez Espinoza F, Mendoza D, et al. Toca 511 gene transfer and treatment with the prodrug, 5-fluorocytosine, promotes durable antitumor immunity in a mouse glioma model. *Neuro-Oncology*. 2017;19:930-939.
28. Qian J, Wang C, Wang B, et al. The IFN-gamma/PD-L1 axis between T cells and tumor microenvironment: hints for glioma anti-PD-1/PD-L1 therapy. *J Neuroinflammation*. 2018;15:290.
29. Hsu J, Hodgins JJ, Marathe M, et al. Contribution of NK cells to immunotherapy mediated by PD-1/PD-L1 blockade. *J Clin Invest*. 2018;128:4654-4668.
30. Dunai C, Murphy WJ. NK cells for PD-1/PD-L1 blockade immunotherapy: pinning down the NK cell. *J Clin Invest*. 2018;128:4251-4253.
31. Kim JE, Patel MA, Mangraviti A, et al. Combination therapy with anti-PD-1, anti-TIM-3, and focal radiation results in regression of murine gliomas. *Clin Cancer Res*. 2017;23:124-136.
32. Kamada T, Togashi Y, Tay C, et al. PD-1(+) regulatory T cells amplified by PD-1 blockade promote hyperprogression of cancer. *Proc Natl Acad Sci USA*. 2019;116:9999-10008.
33. Dovedi SJ, Adlard AL, Lipowska-Bhalla G, et al. Acquired resistance to fractionated radiotherapy can be overcome by concurrent PD-L1 blockade. *Can Res*. 2014;74:5458-5468.
34. Alexandrov LB, Nik-Zainal S, Wedge DC, et al. Signatures of mutational processes in human cancer. *Nature*. 2013;500:415-421.
35. Jiang H, Rivera-Molina Y, Gomez-Manzano C, et al. Oncolytic adenovirus and tumor-targeting immune modulatory therapy improve autologous cancer vaccination. *Can Res*. 2017;77:3894-3907.
36. Chen CY, Hutzen B, Wedekind MF, Cripe TP. Oncolytic virus and PD-1/PD-L1 blockade combination therapy. *Oncolytic Virother*. 2018;7:65-77.
37. Wallin JJ, Bendell JC, Funke R, et al. Atezolizumab in combination with bevacizumab enhances antigen-specific T-cell migration in metastatic renal cell carcinoma. *Nat Commun*. 2016;7:12624.
38. Motz GT, Santoro SP, Wang L-P, et al. Tumor endothelium FasL establishes a selective immune barrier promoting tolerance in tumors. *Nat Med*. 2014;20:607-615.
39. Fujita K, Kato T, Hatano K, et al. Intratumoral and s.c. injection of inactivated hemagglutinating virus of Japan envelope (GEN0101) in metastatic castration-resistant prostate cancer. *Cancer Sci*. 2020;111:1692-1698.
40. Kiyohara E, Tanemura A, Nishioka M, et al. Intratumoral injection of hemagglutinating virus of Japan-envelope vector yielded an antitumor effect for advanced melanoma: a phase I/IIa clinical study. *Cancer Immunol Immunother*. 2020;69:1131-1140.
41. Matsushima-Miyagi T, Hatano K, Nomura M, et al. TRAIL and Noxa are selectively upregulated in prostate cancer cells downstream of the RIG-I/MAVS signaling pathway by nonreplicating Sendai virus particles. *Clin Cancer Res*. 2012;18:6271-6283.
42. Nomura M, Ueno A, Saga K, Fukuzawa M, Kaneda Y. Accumulation of cytosolic calcium induces necroptotic cell death in human neuroblastoma. *Can Res*. 2014;74:1056-1066.

SUPPORTING INFORMATION

Additional supporting information may be found online in the Supporting Information section.

How to cite this article: Sugii N, Matsuda M, Okumura G, et al. Hemagglutinating virus of Japan-envelope containing programmed cell death-ligand 1 siRNA inhibits immunosuppressive activities and elicits antitumor immune responses in glioma. *Cancer Sci*. 2021;112:81–90. https://doi.org/10.1111/cas.14721